Industrial Crops & Products 123 (2018) 315–322

Contents lists available at ScienceDirect

Industrial Crops & Products

journal homepage: www.elsevier.com/locate/indcrop

Sucrose synthase gene expression analysis in the fibre nettle (*Urtica dioica* L.) cultivar "clone 13"

Aurélie Backes[a], Marc Behr[a], Xuan Xu[a], Edoardo Gatti[b], Sylvain Legay[a], Stefano Predieri[b], Jean-Francois Hausman[a], Michael K. Deyholos[c], Giampiero Cai[d], Gea Guerriero[a,*]

[a] Luxembourg Institute of Science and Technology (LIST), Environmental Research and Innovation (ERIN) Department, Esch/Alzette, L-4362, Luxembourg
[b] Institute of Biometeorology (IBIMET), National Research Council, Via P. Gobetti, 101-I, 40129 Bologna, Italy
[c] Department of Biology, University of British Columbia, Kelowna, British Columbia, V1V 1V7, Canada
[d] University of Siena, Department of Life Sciences, Via Pier Andrea Mattioli, 4, 53100, Siena, Italy

ARTICLE INFO

Keywords:
Urtica dioica
Bast fibres
Sucrose synthase
Gene expression analysis
Cell wall biosynthesis

ABSTRACT

The use and valorisation of fibre crops are sustainable solutions to reduce the world's dependence on petroleum-derived products and fossil energy. Fibre crops have a relatively short growth cycle and provide high amounts of biomass used in different industrial sectors. Among fibre crops there is stinging nettle (*Urtica dioica* L.), a perennial herbaceous plant growing in temperate regions. Nettle phloem fibres (a.k.a. bast fibres) have a high cellulose content (ca. 80%) and low amount of lignin (ca. 4%); additionally, they are silky and have a high tensile strength. The gelatinous cell walls of bast fibres are primarily composed of cellulose. The biosynthesis of cellulose is dependent on the provision of uridine diphosphate glucose, which, besides being formed from glucose-1-phosphate through uridine diphosphate glucose pyrophosphorylase, can also be produced via the reaction catalysed by sucrose synthase (*SUS*). A regulation of *SUS* gene expression accompanying the developmental stages of the bast fibres is therefore likely to exist along the stem of nettle plants. The objectives of this study were: 1) to identify the *SUS* genes in nettle and 2) to analyse their differential expression in tissues of stem internodes sampled at different heights (i.e. top, middle and bottom). The gene expression analysis is accompanied by optical and confocal microscopy observations concerning cellulose and lignin distribution. The results here presented identify 6 *SUS* genes in nettle belonging to the three Angiosperm groups previously reported (groups I–III). Their gene expression analysis shows a differential regulation in the stem tissues sampled at different heights, which reflects the increase in cell wall thickness of bast fibres along the stem of nettle. In particular, 3 expression patterns of genes either more expressed in young/old stem regions or peaking at the middle internode are identified with the heat map hierarchical clustering. This is the first study on the expression of *SUS* genes in a nettle fibre variety and on the immunohistochemical analysis of *U. dioica* internodes sampled at different stem heights. This work will serve as a basis for future molecular studies on a neglected, yet potential multi-purpose plant.

1. Introduction

Currently, many studies focus on natural fibres, because of their different industrial applications and their sustainability (Dunne et al., 2016; Guerriero et al., 2017). Fibre crops provide extraxylary fibres, the bast fibres, which mechanically support the phloem. Bast fibres are divided into xylan- and cellulosic-type (a.k.a gelatinous), depending on the composition of their cell walls (Mikshina et al., 2013).

Among the plants supplying cellulosic fibres, there is stinging nettle (*Urtica dioica* L.), a perennial herbaceous plant growing in temperate regions. Even if considered by the traditional agriculture as a weed, stinging nettle has great potential as a fibre crop in the natural textile industry, an industry requiring production by organic methods (Gatti et al., 2008; Hartl and Vogl, 2002). The fibres produced by nettle have hypo-lignified cell walls, they are long, silky, fine and with interesting physicochemical characteristics, such as high tensile strength, thermo-regulatory and low specific weight (Guo et al., 2005; Fischer et al., 2012). Besides fibre production, nettle also provides raw materials of interest for the medicinal, cosmetic and energy sectors (Di Virgilio et al., 2015). These features make this species interesting for potential industrial exploitation as a multi-purpose plant. Nettle stem, like textile hemp (*Cannabis sativa* L.), is composed of a cortex with a lignified core

* Corresponding author.
E-mail address: gea.guerriero@list.lu (G. Guerriero).

https://doi.org/10.1016/j.indcrop.2018.06.090
Received 20 October 2017; Received in revised form 27 June 2018; Accepted 30 June 2018

and cellulosic bast fibres. Nettle bast fibres possess a gelatinous (i.e. cellulosic) tertiary cell wall layer (G-layer) and can attain considerable lengths (Bacci et al., 2009). More than bundles, they form less compact groups of fibres, which make their separation easier.

With the exception of a few studies focusing on the characterisation of nettle fibre yield and composition (Asgarpanah and Mohajerani, 2012), the phenolic compound profiling in different plant organs (Pinelli et al., 2008), the carbohydrate analysis of micro-dissected stem tissues (Angeles et al., 2006) and the assessment of its phytoremediation potential (Viktorova et al., 2016), no detailed molecular analyses are yet available on nettle tissues. A fibre nettle clone ("clone 13") selected in Germany by Bredemann (1959) for its high fibre yield (16%, as compared to 4–5% in wild nettle), shows a significant higher cellulose content in the fibres extracted from the older internodes in the basal portion of the stalk, if compared to the fibres of intermediate and apical internodes (Bacci et al., 2011).

In this study, with the aim of confirming and enriching the knowledge on cellulose and lignin distribution in the stem tissues of nettle, histological and total lignin quantitative analyses were carried out on the fibre nettle "clone 13". Moreover, a targeted gene expression analysis was performed to investigate the mechanisms associated to the reported gradient in cellulose content in the fibres of "clone 13″ (Bacci et al., 2011). Six glycosyltransferase (GT) genes which code for sucrose synthases (*SUS*) involved in the provision of the nucleotide sugars (UDP-glucose) needed for cellulose biosynthesis, were here identified. We provide the gene expression analysis in different tissues and organs (stem core and cortex, leaves, roots) of 5 weeks-old nettle plants. We also identify, for the first time, the most suitable reference genes for data normalization in nettle. To our knowledge, this is the first study identifying and analysing the gene expression profile of *SUS* from the fibre nettle cultivar "clone 13".

Considering the importance of fibre crops for the provision of biomass used by different industries (e.g. textile, construction, biocomposite, paper), this study aims at valorising nettle. In particular, we wish to draw the attention of the scientific community on the suitability of *U. dioica* as a model for fundamental studies centred on bast fibre development and cellulose biosynthesis. On a longer term perspective, this work wants to propose this overlooked plant as a promising candidate for the diversification of the current bast fibre market.

2. Material and methods

2.1. Plant growth

In this study, the fibre nettle cultivar "clone 13" of the Bredemann selection was used because of its high fibre yield (Bacci et al., 2011). *U. dioica* plants were propagated using stem cuttings of a "clone 13" mother plant and grown in controlled conditions in 2 incubators (20 plants in each incubator) following a cycle of 16 h light 25 °C/ 8 h dark 20 °C. After 5 weeks of growth, samples were taken along three regions of the stem localized at different heights (i.e. top, middle and bottom), following the same sampling strategy described for textile hemp by our group (Guerriero et al., 2017; Mangeot-Peter et al., 2016). The "TOP" segment is the internode located at the top (below the apex). The "MID" (middle) segment shows a kink when tilted and therefore possibly contains the so-called snap point, a region marking the transition from elongation to fibre thickening and resulting in changes in fibre mechanical properties (Guerriero et al., 2017; Gorshkova et al., 2003). The actual presence of the snap point in the "MID" internode of nettle awaits further cytological confirmation. The "BOT" (bottom) segment corresponds to the second internode below the "MID". Four biological replicates were used, each consisting of 7 nettle plants selected among the 2 incubators (only plants showing the same height were used for this study). A segment of 2.5 cm was collected from the central portion of each internode, to avoid variations in gene expression due to the differences in developmental stages of the cell types (as described in textile hemp by Guerriero et al., 2017). Each internode was peeled to separate the cortex from the core, as previously described in hemp (Mangeot-Peter et al., 2016). All collected samples were frozen in liquid nitrogen and stored at –80 °C until analysis.

2.2. (Immuno)histochemical analyses

Sample preparation for immunohistochemical analysis with the CBM3a recombinant protein (PlantProbes, UK) was carried out as previously described (Behr et al., 2016). Sections of ca. 5 mm, sampled from the middle of each internode, were impregnated under vacuum in sodium phosphate buffer (0.2 M, pH 7.2) with glutaraldehyde (1%), paraformaldehyde (2%) and caffeine (1 g). Samples were then fixed overnight at 4 °C and dehydrated in ethanol series (70% – 30 min, 70% – 60 min, 95% – 30 min, 95% – 60 min, 100% – 30 min). The samples were subsequently embedded in resin containing PEG 400 (2% v/v) and dimethacrylate ethylene glycol (0.4% w/v) and finally included (Technovit® 7100, Heraeus Kulzer GmbH), following the manufacturer's instructions. The recombinant crystalline cellulose-binding module CBM3a (Plant Probes) was used at 10 µg/mL in milk protein/PBS (phosphate buffered saline). Sections were incubated 1.5 h with the CBM3a recombinant protein, then washed 3 times for 10 min in PBS and incubated with mouse anti-His monoclonal antibody (1% in MP/PBS, Sigma). The slices were rinsed for three times in PBS as previously described and finally incubated in 50-fold diluted anti-mouse IgG coupled to FITC (Sigma). Images were acquired with a confocal microscope LSM 510 Meta (Zeiss), by using the following settings: excitation at 488 nm, filter HFT 488/594 and emission recorded with LP 505. The Mäule staining was performed on fresh sections cut manually (as is the case for the "TOP" internode) or with a vibratome (sections of "MID" and "BOT" internodes embedded in 5% agarose). Sections were incubated in potassium permanganate solution at 1% (w/v) for 5 min, rinsed with pure water, washed with 3.6% hydrochloric acid and mounted in saturated ammonia solution for immediate observation with an optical microscope. Cross sections obtained with the microtome were incubated for 15 min in the FASGA solution (Tolivia and Tolivia, 1987) at 55 °C, rinsed with pure water and observed with an optical microscope (Leica DMR).

2.3. Total lignin content in the core tissues of the stem

The quantification of total lignin was carried out as described previously (Behr et al., 2018) with some modifications concerning the cell wall residue (CWR) preparation. CWR was obtained by washing the powdered plant material first with 70% ethanol three times, followed by washing with acetone and methanol. All washing steps were performed at room temperature with agitation for 15 min. Total lignin was determined by using the acetyl bromide protocol as described by Behr et al. (2018).

2.4. RNA extraction and cDNA synthesis

Samples were crushed to a fine powder using a mortar and a pestle in liquid nitrogen. Total RNA was extracted using the RNeasy Plant Mini Kit (Qiagen, Leusden, Netherlands) according to the manufacturer's instructions (including the on-column digestion with DNase I). RNA quality and quantity were assessed with a NanoDrop ND-1000 spectrophotometer (Thermo Scientific, Villebon-sur-Yvette, France) and a 2100 Bioanalyzer (Agilent, Santa Clara, CA, USA). All the RNAs displayed a RIN above 8. In case of 230 nm contamination (ratio 260/

Table 1
List of primers used in the study with details on the amplicon length, Tm, PCR efficiency and regression coefficient.

Name	Sequence (5' → 3')	Amplicon Length (bp)	Amplicon Tm	PCR Efficiency (%)	Regression Coefficient (R^2)
Histone 3 Fwd	AGGAAGATGGCAAGCTGAAG	93	81.79	96	0.997
Histone 3 Rev	ATTGCACACAGCATCGAGTC				
EF 2 Fwd	AGAGTTGCGTCGGATTATGG	128	83	93	0.997
EF 2 Rev	CTTCTTGGGCAATGATACCC				
Actin Fwd	TCCGATTTACGAGGGTTACG	98	81	95	0.999
Actin Rev	GCTCCGTCAGGATTTTCATC				
eTIF4E Fwd	AGGTGAGCATTGGGAAACAG	103	80.32	97	0.992
eTIF4E Rev	TTCTTGGCACCCCTATCAAG				
TIP 41 Fwd	TCCCCAACCCTTAAACTGTG	71	77.7	93	0.997
TIP 41 Rev	CTTTCCCCAAACACCATCTC				
Tubulin Fwd	GGGCTTCTTGGTCTTCAATG	80	84.3	95	0.996
Tubulin Rev	TCGACAGACAAACGTTCGAG				
CDPK Fwd	GATGTGGATGGGAATGGAAC	143	82.46	99	0.999
CDPK Rev	TCGTCTCGGGTGATAAATCC				
RAN Fwd	AAGAGCGGACGAAGAATACG	93	81.9	91	0.995
RAN Rev	CGAGTGAATCGGGAAAGAAG				
Cyclo Fwd	TTGGAGCCCTGAGACAATTC	99	79.8	111	0.996
Cyclo Rev	ACGGAGGTTTTGCACTTCAC				
SUS1 Fwd	CAAGGACAACGAGGAAAAGG	137	84.3	89	0.997
SUS1 Rev	TCGCAGATGTGACGGTAAAG				
SUS2 Fwd	GAAGGCGAAGCATTTACTCG	123	83.2	97	0.987
SUS2 Rev	AAGCTCTCGGCCACAATAAG				
SUS3 Fwd	GCAACCTCACACATTGTTGG	123	83.2	99	0.997
SUS3 Rev	GGCAGAATTATGGCTTCCTG				
SUS4 Fwd	TCGAGCACAAGTTTCGAGAG	79	85.2	93	0.997
SUS4 Rev	AGGCTAATCATGCCGAGAAC				
SUS5 Fwd	ATCATCGTTGATGGGCTCTC	101	83.5	105	0.997
SUS5 Rev	GGATCGAGCTTGCATTTCTC				
SUS6 Fwd	ACCCCAATCACTGGAACAAG	87	80.7	90	0.991
SUS6 Rev	ACACCTTCGTCGCGTAAATC				

230 < 2), samples were cleaned with ammonium acetate (NH_4OAc) and then washed in ethanol. One microgram of RNA was retro-transcribed using the ProtoScript II RTase (NEB), following the manufacturer's instructions.

2.5. Gene identification and primer design

The sequences of the six predicted nettle *SUS* genes were retrieved by blasting the *Arabidopsis SUS* against the available nettle leaf database at Blast4OneKP (http://db.cngb.org/blast4onekp/home). Nine candidate reference genes (i.e. tubulin, actin, the translation elongation factor *EF2*, the eukaryotic translation initiation factor *eTIF4E*, cyclophilin, the tonoplast intrinsic protein *TIP41*, histone3, the gene coding for small GTP-binding protein *RAN*, the gene corresponding to the calcium-dependent protein kinase *CDPK*) chosen from the list of genes reported in textile hemp (Mangeot-Peter et al., 2016), were validated in this study. The sequences of the *SUS* and the candidate reference genes are listed in Supplementary file 1. Specific gene primers were designed using "Primer3Plus" (http://www.bioinformatics.nl/cgi-bin/primer3plus/primer3plus.cgi) and checked using the software OligoAnalyzer 3.1 tool from Integrated DNA technologies (http://eu.idtdna.com/calc/analyzer). Primer efficiencies were calculated by RT-qPCR using six serial dilutions of cDNA (10, 2, 0.4, 0.08, 0.016, 0.0032 ng/µL). The list of primers is given in Table 1.

2.6. Quantitative real-time PCR and statistical analysis

For the RT-qPCR analysis, the reactions were performed in 384-well plates using a liquid handling robot (epMotion 5073, Eppendorf, Hamburg, German). The cDNA was amplified using the SYBRGreen qPCR Master Mix. The reactions were run in technical triplicates using the cycling parameters and melt curve analysis described previously (Mangeot-Peter et al., 2016). Gene expression was calculated using qbase + version 3.1 (Biogazelle, Zwijnaarde, Belgium, www.qbaseplus.com); normalization was carried out using tubulin and RAN which geNorm™ identified as sufficient among the 5 most stable candidates (i.e. cyclophilin, *EF2*, *eTIF4E*, *RAN* and tubulin). Statistics was performed from log2 transformed data using a one-way ANOVA with a Tukey-Kramer post-hoc test, as implemented in qbase+ (Hellemans et al., 2007). A hierarchical clustering using Pearson correlation and complete linkage was used to generate groups with similar expression patterns in Cluster 3.0 (correlation threshold = 0.95) (Eisen et al., 1998) and the heat map was generated with Java TreeView (Saldanha, 2004), available at http://jtreeview.sourceforge.net/.

2.7. Phylogenetic tree

The maximum likelihood phylogenetic analysis was carried out on different *SUS* from the following species: *Arabidopsis thaliana* (Bieniawska et al., 2007), *Theobroma cacao* (Li et al., 2015), *Linum usitatissimum*, *Populus trichocarpa* (An et al., 2014), *Gossypium raimondii* (Zou et al., 2013), *Oryza sativa*, *Vitis vinifera* (Zhu et al., 2017), *Nitrosomonas europaea*, *Acidithiobacillus caldus*, *Denitrovibrio acetiphilus*, *Melioribacter roseus*, *Pinus taeda*, *Ananas comosus*, *Eucalyptus grandis*, *Malus* x *domestica*, *Prunus persica*, *Coccomyxa subellipsoidea, Ginkgo biloba* and *Picea abies.* The tree was built with PhyML (Guindon and Gascuel, 2003) (available at: http://www.phylogeny.fr) and viewed with iTOL (http://itol.embl.de). The sequences of *SUS* from *A. thaliana*, *L. usitatissimum*, *V. vinifera*, *A. comosus*, *T. cacao*, *O. sativa E. grandis*, *M.* x *domestica*, *P. persica*, *P. trichocarpa*, *C. subellipsodea*, were retrieved by querying the Phytozome portal (https://phytozome.jgi.doe.gov/pz/portal.html); the *SUS* from *P. taeda* and *P. abies* were obtained by blasting against the Congenie database (http://congenie.org/blast). The *SUS* from *G. raimondii* were retrieved at Cottongen (https://www.

Table 2
List of the SUS protein accession numbers from different species used in this study.

Species	Protein id	Accession number
Dicots		
Arabidopsis thaliana	AtSUS1	AT5G20830.1
	AtSUS2	AT5G49190.1
	AtSUS3	AT4G02280.1
	AtSUS4	AT3G43190.1
	AtSUS5	AT5G37180.1
	AtSUS6	AT1G73370.1
Urtica dioica	UdSUS1	WKCY2009983
	UdSUS2	WKCY2049848
	UdSUS3	WKCY2014176
	UdSUS4	WKCY2001666
	UdSUS5	WKCY2048067
	UdSUS6	WKCY2015371
Eucalyptus grandis	EgSUS2	Eucgr.B01577.1
	EgSUS5	Eucgr.J01640.1
	EgSUS6	Eucgr.K02305.1
Gossypium raimondii	GrSUS1	Gorai.009G038000.1
	GrSUS2	Gorai.004G142700.1
	GrSUS3	Gorai.010G092300.1
	GrSUS4	Gorai.010G091800.1
	GrSUS5	Gorai.001G083400.1
	GrSUS6	Gorai.007G047100.1
	GrSUS7	Gorai.013G222400.1
Populus trichocarpa	PtrSUS2	Potri.014G126800.1
	PtrSUS4	Potri.015G029100.1
	PtrSUS5	Potri.004G081300.1
	PtrSUS6	Potri.002G195500.1
Theobroma cacao	TcSUS1	Thecc1EG037468t1
	TcSUS2	Thecc1EG021253t1
	TcSUS3	Thecc1EG004698t1
	TcSUS4	Thecc1EG037464t1
	TcSUS5	Thecc1EG017585t2
	TcSUS6	Thecc1EG013507t1
Linum usitatissimum	LuSUS1	Lus10020506
	LuSUS2	Lus10013417
	LuSUS3	Lus10007372
	LuSUS4	Lus10017984
	LuSUS5	Lus10020791
	LuSUS6	Lus10041979
Vitis vinifera	VvSUS1	GSVIVT01035210001
	VvSUS2	GSVIVT01035106001
	VvSUS3	GSVIVT01028043001
	VvSUS4	GSVIVT01015018001
	VvSUS5	GSVIVT01029388001
Prunus persica	PpSUS1	Prupe.2G242300.1
	PpSUS2	Prupe.1G131700.1
	PpSUS5	Prupe.3G014100.1
	PpSUS6	Prupe.5G241700.1
Malus x domestica	MdSUS1	MDP0000872262
	MdSUS2	MDP0000859573
	MdSUS5	MDP0000195934
	MdSUS6	MDP0000212593
Monocots		
Oryza sativa	OsSUS1	LOC_Os04g24430.1
	OsSUS2	LOC_Os03g22120.1
	OsSUS3	LOC_Os03g28330.4
	OsSUS4	LOC_Os04g17650.1
	OsSUS5	LOC_Os06g09450.2
	OsSUS6	LOC_Os02g58480.1
Ananas comosus	AncSUS3	Aco006349.1
	AncSUS6	Aco009217.1
Gymnosperms		
Pinus taeda	PtSUS	PITA_000044298-RA
Ginkgo biloba	GbSUS	gba_locus_4197
Picea abies	PaSUS	MA_10432094g0010
Bacteria		
Nitrosomonas europaea	NeSUS	WP_011111802.1
Acidothiobacillus caldus	AcSUS	WP_004872341.1
Denitrovibrio acetiphilus	DaSUS	WP_013012179.1
Melioribacter roseus	MrSUS	WP_014855986.1
Green algae		
Coccomyxa subellipsoidea	CsSUS	XP_005643464.1

cottongen.org/analysis/50), while *G. biloba SUS* at the Medicinal Plant Genomics Resource (MPGR; http://medicinalplantgenomics.msu.edu/). The protein id and the accession numbers are indicated in Table 2.

3. Results and discussion

3.1. Microscopic analysis of the nettle stem

Histological analyses carried out on nettle stem cross sections stained with the Mäule reagent revealed an increasing signal (the red colour is indicative of S-lignin) from the top to the bottom of nettle stems (Fig. 1A–C and inset). This increase in the intensity of the signal is accompanied by a more developed vascular tissue, with vessels displaying a wider lumen (Fig. 1C, inset). At the bottom of the stem, the bast fibres showed an increase in the cell wall thickness (Fig. 1C, inset). These results confirm previous quantitative analysis of cellulose content in the fibres of "clone 13", where significant higher percentages were found at the bottom if compared to the middle and top, while no statistically significant differences in hemicellulose content were measured at the different stem heights (Bacci et al., 2009). Moreover, our results suggest that the nettle stem is a valid model to study the stages accompanying bast fibre differentiation, in a manner analogous to what was previously shown in textile hemp (Guerriero et al., 2017; Mangeot-Peter et al., 2016).

Resin-embedded microscope sections stained with FASGA (which enables the differentiation of cellulose and lignin on the basis of a blue and red coloration, respectively) confirmed the presence of thick cellulosic cell walls in the bast fibres at the bottom of the stem (Fig. 1D–F). More specifically, the xylem tissue shows a progressive increase in vessel sizes and in woody fibre number from the top to the bottom; the bast fibres at the top and the middle show thin cell walls, while at the bottom they display thick gelatinous cell walls.

The quantification of total lignin using the acetyl bromide method revealed a statistically-significant decrease at the "BOT" with respect to the "TOP" and "MID" (*p*-value "BOT" *vs* "TOP": 7,11479E-05; *p*-value "BOT" *vs* "MID": 0.000176) (Table 3). While the acetyl bromide method remains the technique of choice to quantify total lignin from small quantities of starting material (Moreira-Vilar et al., 2014), the potential interference caused by furfural originating from the xylose in hemicelluloses (xyloglucan and xylan) has to be taken into account (Hatfield et al., 1999). The higher absorbance (and consequently higher lignin %) recorded in internodes at the "TOP" and "MID" may be partly due to the presence of furfural derived from hemicelluloses (notably xyloglucan, the chief hemicellulose in dicots' primary walls).

The immunohistochemical analysis carried out with the CBM3a recombinant protein recognizing crystalline cellulose confirmed the presence of bast fibres with a thick cellulosic cell wall at the bottom of the stem (Fig. 2C and D). At the top and middle internode, a ring of faintly stained developing bast fibres is present (Fig. 2A and B); in the same sections, the developing xylem vessels are strongly cross-reacting with the recombinant protein. At the bottom, files of xylem fibres form a continuous ring connecting the vessels. It should be noted that our immunohistochemical analyses on the nettle bast fibres are in agreement with the previously reported bast fibre thicknesses along the nettle stem (19, 32, 47 μm at the top, middle and bottom) (Bacci et al., 2009).

Differently from hemp, the bast fibres of nettle are more loosely arranged and do not form bundles, moreover they are not round, but appear pentagonal/hexagonal in transversal cross-section (Fig. 2D arrow). At this stage, we cannot rule out the presence of secondary bast fibres: smaller fibres are present, however the FASGA staining did not detect the presence of more lignin, with respect to the fibres displaying a wider lumen (as is the case with hemp secondary bast fibres) (Fig. 1F). Further cytological and immunohistochemical analyses will clarify this aspect.

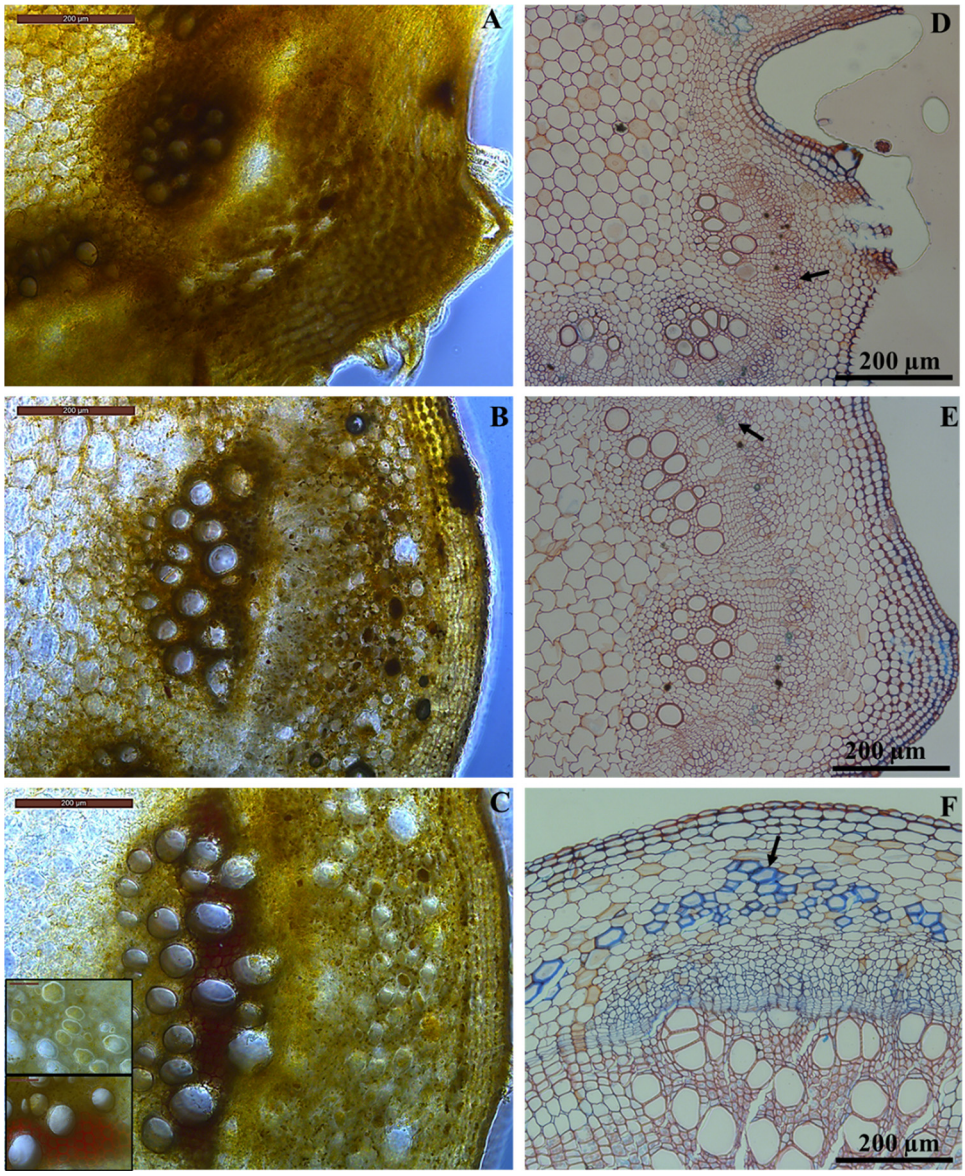

Fig. 1. Staining with Mäule reagent (A–C) and FASGA (D–F) of nettle stem cross sections corresponding to internodes sampled at the top (A–D), middle (B–E) and bottom (C–F). The insets in C show magnified details of bast fibres (no signal) and xylem tissue (strong red coloration). The sections in A-B-C are agarose embedded; A is manually cut, while B and C are cut with a vibratome. The sections in D-E-F are resin embedded and cut with a microtome. Lignin is stained in red, while cellulose in blue. Arrows indicate bast fibres. Bars are 200 µm in all the panels (For interpretation of the references to colour in this figure legend, the reader is referred to the web version of this article).

Table 3
Lignin percentages (± standard deviation) in the fibres and lignin content in the core of internodes sampled at the top, middle and bottom. The results previously reported by Bacci et al. (2009) are provided for a comparison between stem tissues.

	"TOP" FIBRES	"MID" FIBRES	"BOT" FIBRES	Reference
Lignin %	3.5±0.2	3.8±0.9	4.4±0.4	Bacci et al. (2009)
	"TOP" CORE	"MID" CORE	"BOT" CORE	Reference
Lignin %	5.9 ± 0.18	5.9 ± 0.39	4.1 ± 0.2	This study

3.2. Identification of SUS genes in stinging nettle

The gradient of cellulose content in the bast fibres evidenced by immunohistochemistry (Figs. 1 and 2) and, previously, by quantitative analyses (Bacci et al., 2009), was further investigated in this study through *SUS* gene expression profiling at different stem heights. BLASTP analyses carried out at Blast4OneKP using the thale cress *SUS* protein sequences (6 proteins in total) led to the identification of 6 *SUS* in stinging nettle (hereafter referred to as UdSUS1-6 for the protein sequences and *UdSUS1-6* for the genes). Of these sequences, 2 are complete (i.e. UdSUS3 and UdSUS6, Supplementary file 1), as both the start and stop codons are present.

The maximum likelihood phylogenetic analysis performed using *SUS* full length protein sequences from different Angiosperms, both monocots and dicots, Gymnosperms, as well as from bacteria and green algae, resulted in the clustering of the 6 nettle *SUS* across the three Angiosperm groups previously reported (groups I–III) (Zhang et al., 2013). The phylogenetic tree shows that the plant *SUS* form a monophyletic group, a result which was already previously described (Zhu et al., 2017): this shows that plant *SUS* originated from a common ancestor. More specifically, in the plant *SUS* group, 2 nettle *SUS*, UdSUS1-4, belong to group I, UdSUS3 is in group II, and UdSUS2-5-6 are in group III (Fig. 3). Within each group of *SUS*, the monocots form always separate branch (Fig. 3). The *SUS* from the Gymnosperms here

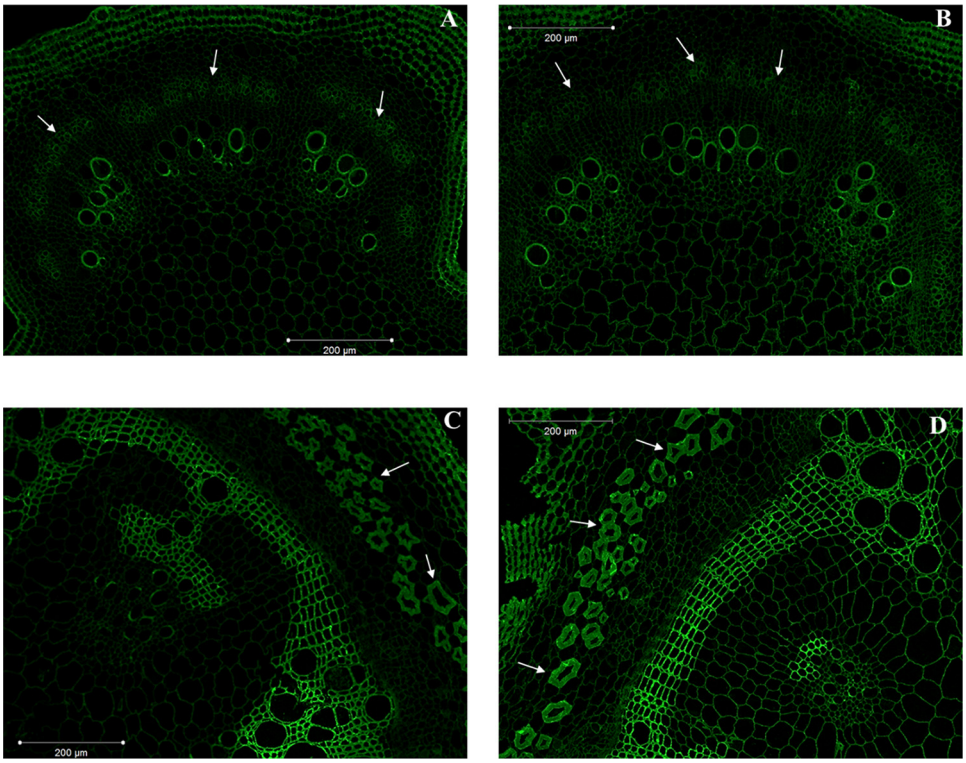

Fig. 2. Immunodetection of crystalline cellulose of nettle stem cross sections corresponding to internodes sampled at the top (A), middle (B) and bottom (C–D).

analysed cluster together in a sister group to the *SUS* of groups I and II (Fig. 3).

3.3. Expression patterns of SUS in nettle stem tissues, roots and leaves

According to the heat map hierarchical clustering of expression profiles (Fig. 4), it is possible to identify 3 different *SUS* expression patterns in the stems of stinging nettle. The first group is represented by *UdSUS1* and *UdSUS4*, which cluster together and are characterized by an increasing expression from the top to the bottom of the stem core; in the stem cortex, notably, they peak at the middle (Figs. 4 and 5 and Table 4). The middle internode sampled in this study probably contains the snap point, as by bending the stem, a kink is observed in this internode, indicative of a shift in the mechanical properties of the bast fibre cell walls. Therefore, a peak in expression of *UdSUS1* and *UdSUS4* may reflect a role of these genes in the transition from intrusive growth to cell wall thickening.

UdSUS3 forms a separate group and its expression in the core and stem cortex is the highest at the bottom (Figs. 4 and 5 and Table 4). The last group is formed by *UdSUS2*, *UdSUS5* and *UdSUS6* which decrease in expression from the top to the bottom of the core, while they increase basipetally, in the cortical tissues (Figs. 4 and 5 and Table 4). This is indicative of a possible function for these genes in the metabolism linked to cell wall thickening in the bast fibres.

As compared to the leaves, only *UdSUS1* and *UdSUS4* show statistically significant higher expressions in the roots (Fig. 5): this finding may indicate a role of these genes in the metabolism of sink tissues. *UdSUS3* is the gene with the highest expression in the leaves (Figs. 4 and 5 and Table 4), however it is also expressed in the roots, therefore it may represent a constitutive-type of gene linked to the basal

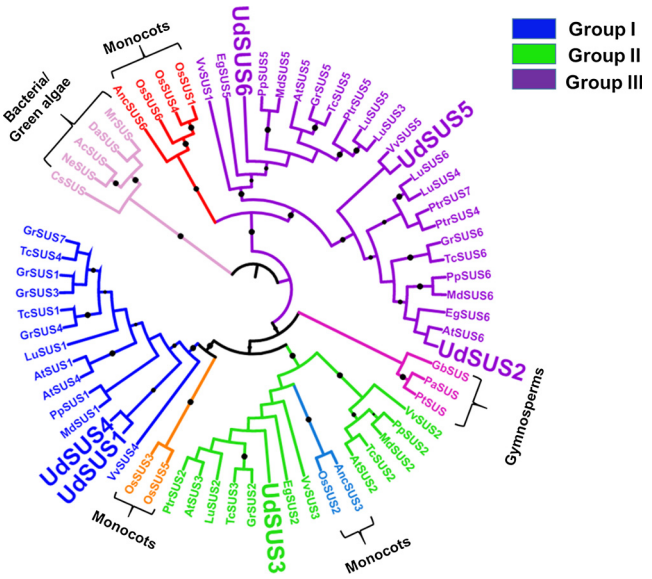

Fig. 3. Maximum likelihood phylogenetic tree (bootstraps: 100) of sucrose synthases of *A. thaliana* (At), *U. dioica* (Ud), *T. cacao* (Tc), *L. usitatissimum* (Lu), *P. trichocarpa* (Ptr), *G. raimondii* (Gr), *O. sativa* (Os), *V. vinifera* (Vv), *N. europaea* (Ne), *A. caldus* (Ac), *D. acetiphilus* (Da), *M. roseus* (Mr), *P. taeda* (Pt), *A. comosus* (Anc), *E. grandis* (Eg), *M.* x *domestica* (Md), *P. persica* (Pp), *C. subellipsodea* (Cs), *G. biloba* (Gb) and *P. abies* (Pa). The protein accession numbers are indicated in Table 2. Bootstraps > 80% are indicated as black circles on the branches. The bigger the circle size, the higher the bootstrap value.

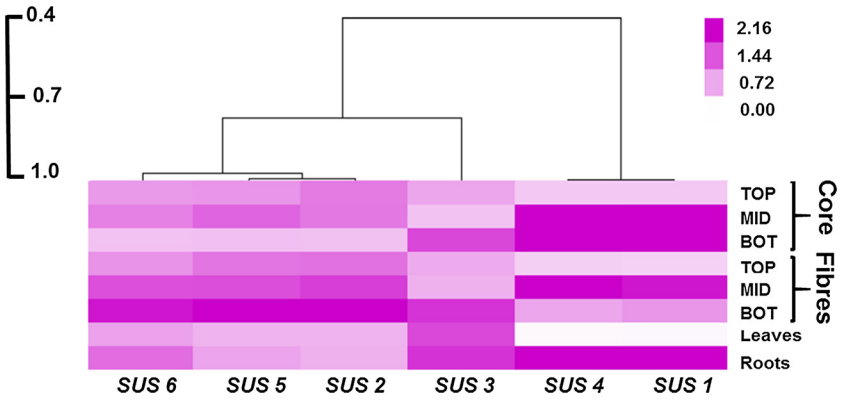

Fig. 4. Heatmap hierarchical clustering with correlation bar of *SUS* expression profiles in the different tissues of *U. dioica*. The heat map hierarchical clustering was obtained using a Pearson's rank correlation coefficient and complete linkage.

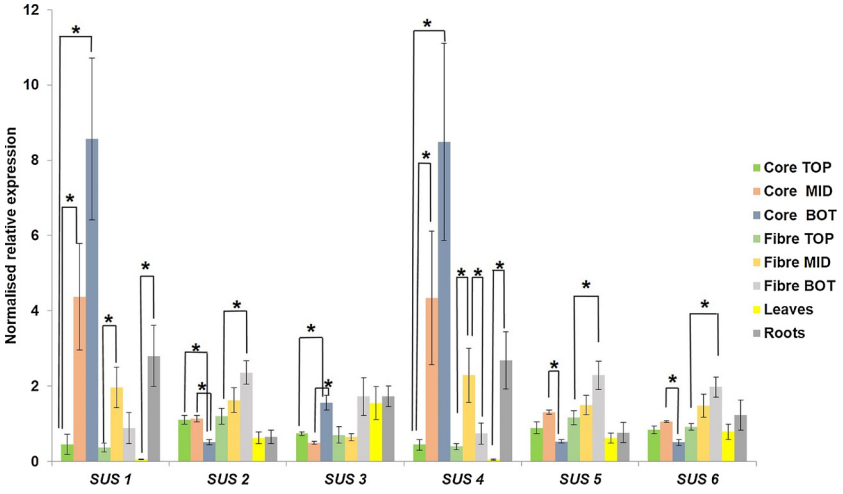

Fig. 5. Normalized relative expression of sucrose synthase genes in different tissues of *U. dioica*. Asterisks denote significant differences at the one-way ANOVA test ($p < 0.05$).

Table 4
Expression values (expressed as normalized relative quantities) of SUS in the different nettle tissues. Different letters indicate statistically different values ($p < 0.05$) at the one-way ANOVA test with a Tukey-Kramer post-hoc test.

	SUS 1	*SUS 2*	*SUS 3*	*SUS 4*	*SUS 5*	*SUS 6*
Core TOP	0.45 ± 0.27 b	1.11 ± 0.11 b	0.74 ± 0.05 a	0.44 ± 0.14 b	0.89 ± 0.16 ab	0.84 ± 0.10 ab
Core MID	4.37 ± 1.41 d	1.14 ± 0.08 b	0.49 ± 0.04 a	4.34 ± 1.77 d	1.31 ± 0.05 b	1.06 ± 0.03 b
Core BOT	8.567 ± 2.15 d	0.51 ± 0.07 a	1.56 ± 0.19 b	8.48 ± 2.62 d	0.53 ± 0.05 a	0.51 ± 0.08 a
Fibre TOP	0.37 ± 0.11 b	1.2 ± 0.21 b	0.7 ± 0.22 a	0.39 ± 0.08 b	1.16 ± 0.19 b	0.92 ± 0.09 b
Fibre MID	1.96 ± 0.54 c	1.63 ± 0.33 bc	0.65 ± 0.09 a	2.29 ± 0.72 c	1.49 ± 0.26 bc	1.48 ± 0.31 bc
Fibre BOT	0.88 ± 0.41 bc	2.36 ± 0.32 c	1.72 ± 0.50 b	0.74 ± 0.28 b	2.29 ± 0.37 c	1.98 ± 0.26 c
Leaves	0.05 ± 0.01 a	0.63 ± 0.16 a	1.54 ± 0.44 b	0.05 ± 0.01 a	0.62 ± 0.13 a	0.79 ± 0.20 a
Roots	2.8 ± 0.81 c	0.65 ± 0.18 a	1.73 ± 0.28 b	2.69 ± 0.76 c	0.77 ± 0.27 a	1.23 ± 0.39 a

metabolism of the plant. *UdSUS1* and *UdSUS4*, as well as *UdSUS2* and *UdSUS5*, show expression patterns that are identical (Figs. 4 and 5 and Table 4); given their incomplete nucleotide sequences, we cannot exclude the possibility that *UdSUS1-UdSUS4* and *UdSUS2-UdSUS5* are the same genes.

4. Conclusions

In this study we perform for the first time histochemical analyses on internodes sampled at different stem heights in nettle. The results enrich previously published quantitative data on cellulose and lignin in the nettle stem. Additionally, we report the presence of 6 *SUS* genes in the fibre nettle cultivar "clone 13" after searching the available database. These genes belong to the previously identified Angiosperm groups (group I–III). We identify *SUS* genes associated with specific stages of bast fibre development and secondary growth. In this respect, it will be interesting to further characterize *UdSUS1* and *UdSUS4*, since their expression peaks at the middle, which is the internode potentially containing the snap point. We additionally provide, for the first time, a list of potential reference genes for expression data normalization in nettle tissues and organs and identify the most stable ones.

Our study paves the way to future bast fibre-oriented molecular analyses on one of the most undervalued fibre-producing plants. Nettle can contribute to the diversification of the current fibre crop market, as it holds the potential to become a multipurpose species with applications in the textile, biocomposite and medicinal sector, besides being an interesting silage cattle feed crop.

Acknowledgements

GG acknowledges the Fonds National de la Recherche, Luxembourg (Project CABERNET C16/SR/11289002) for financial support. The authors thank Camille Renault and Laurent Solinhac for their technical support.

Appendix A. Supplementary data

Supplementary material related to this article can be found, in the online version, at doi:https://doi.org/10.1016/j.indcrop.2018.06.090.

References

An, X., Chen, Z., Wang, Jingcheng, Ye, M., Ji, L., Wang, Jia, Liao, W., Ma, H., 2014. Identification and characterization of the *Populus* sucrose synthase gene family. Gene 539, 58–67. http://dx.doi.org/10.1016/j.gene.2014.01.062.

Angeles, G., Berrio-Sierra, J., Joseleau, J.-P., Lorimier, P., Lefèbvre, A., Ruel, K., 2006. Preparative laser capture microdissection and single-pot cell wall material preparation: a novel method for tissue-specific analysis. Planta 224, 228–232. http://dx.doi.org/10.1007/s00425-006-0285-1.

Asgarpanah, J., Mohajerani, R., 2012. Phytochemistry and pharmacologic properties of *Urtica dioica* L. J. Med. Plants Res. 6, 5714–5719. http://dx.doi.org/10.5897/JMPR12.540.

Bacci, L., Baronti, S., Predieri, S., di Virgilio, N., 2009. Fiber yield and quality of fiber nettle (*Urtica dioica* L.) cultivated in Italy. Ind. Crops Prod. 29, 480–484. http://dx.doi.org/10.1016/j.indcrop.2008.09.005.

Bacci, L., Di Lonardo, S., Albanese, L., Mastromei, G., Perito, B., 2011. Effect of different extraction methods on fiber quality of nettle (*Urtica dioica* L.). Text. Res. J. 81, 827–837. http://dx.doi.org/10.1177/0040517510391698.

Behr, M., Legay, S., Žižková, E., Motyka, V., Dobrev, P.I., Hausman, J.-F., Lutts, S., Guerriero, G., 2016. Studying secondary growth and bast fiber development: the hemp hypocotyl peeks behind the wall. Front. Plant Sci. 7. http://dx.doi.org/10.3389/fpls.2016.01733.

Behr, M., Sergeant, K., Leclercq, C.L., Planchon, S., Guignard, C., Lenouvel, A., Renaut, J., Hausman, J.-F., Lutts, S., Guerriero, G., 2018. Insights into the molecular regulation of monolignol-derived product biosynthesis in the growing hemp hypocotyl. BMC Plant Biol. 18, 1. http://dx.doi.org/10.1186/s12870-017-1213-1.

Bieniawska, Z., Paul Barratt, D.H., Garlick, A.P., Thole, V., Kruger, N.J., Martin, C., Zrenner, R., Smith, A.M., 2007. Analysis of the sucrose synthase gene family in *Arabidopsis*. Plant J. Cell Mol. Biol. 49, 810–828. http://dx.doi.org/10.1111/j.1365-313X.2006.03011.x.

Bredemann, G., 1959. Die große Brennessel *Urtica dioica* L. Forschung über ihren Anbau zur Fasergewinnung. Akademieverlag, Berlin, Germany.

Di Virgilio, N., Papazoglou, E.G., Jankauskiene, Z., Di Lonardo, S., Praczyk, M., Wielgusz, K., 2015. The potential of stinging nettle (*Urtica dioica* L.) as a crop with multiple uses. Ind. Crops Prod. 68, 42–49. http://dx.doi.org/10.1016/j.indcrop.2014.08.012.

Dunne, R., Desai, D., Sadiku, R., Jayaramudu, J., 2016. A review of natural fibres, their sustainability and automotive applications. J. Reinf. Plast. Comp. 35, 1041–1050. http://dx.doi.org/10.1177/0731684416633898.

Eisen, M.B., Spellman, P.T., Brown, P.O., Botstein, D., 1998. Cluster analysis and display of genome-wide expression patterns. Proc. Natl. Acad. Sci. U. S. A. 95, 14863–14868.

Fischer, H., Werwein, E., Graupner, N., 2012. Nettle fibre (Urtica dioica L.) reinforced poly(lactic acid): a first approach. J. Compos. Mater. 46, 3077–3087. http://dx.doi.org/10.1177/0021998311435676.

Gatti, E., Di Virgilio, N., Baronti, S., Bacci, L., 2008. Development of Urtica dioica L. propagation methods for organic production of fiber. In: 16th IFOAM Organic World Congress. June 16–20, Modena, Italy.

Gorshkova, T.A., Salnikov, V.V., Chemikosova, S.B., Ageeva, M.V., Pavlencheva, N.V., van Dam, J.E.G., 2003. The snap point: a transition point in Linum usitatissimum bast fiber development. Ind. Crops Prod. 18, 213–221. http://dx.doi.org/10.1016/S0926-6690(03)00043-8.

Guerriero, G., Behr, M., Legay, S., Mangeot-Peter, L., Zorzan, S., Ghoniem, M., Hausman, J.-F., 2017. Transcriptomic profiling of hemp bast fibres at different developmental stages. Sci. Rep. 7, 4961. http://dx.doi.org/10.1038/s41598-017-05200-8.

Guindon, S., Gascuel, O., 2003. A simple, fast, and accurate algorithm to estimate large phylogenies by maximum likelihood. Syst. Biol. 52, 696–704.

Guo, Y., Wu, H., Sun, X., Qian, X., Shen, Y., 2005. Analysis on the properties of nettle fiber. J. Text. Res. 26, 27–28.

Hartl, A., Vogl, C.R., 2002. Dry matter and fibre yields, and the fibre characteristics of five nettle clones (*Unica dioica L.*) organically grown in Austria for potential textile use. Amer. J. Alternative Agrie. 17, 195–200.

Hatfield, R.D., Grabber, J., Ralph, J., Brei, K., 1999. Using the acetylbromide assay to determine lignin concentrations in herbaceous plants: some cautionary notes. J. Agric. Food Chem. 47, 628–632. http://dx.doi.org/10.1021/jf9808776.

Hellemans, J., Mortier, G., De Paepe, A., Speleman, F., Vandesompele, J., 2007. qBase relative quantification framework and software for management and automated analysis of real-time quantitative PCR data. Genome Biol. 8, R19. http://dx.doi.org/10.1186/gb-2007-8-2-r19.

Li, F., Hao, C., Yan, L., Wu, B., Qin, X., Lai, J., Song, Y., 2015. Gene structure, phylogeny and expression profile of the sucrose synthase gene family in cacao (*Theobroma cacao* L.). J. Genet. 94, 461–472.

Mangeot-Peter, L., Legay, S., Hausman, J.-F., Esposito, S., Guerriero, G., 2016. Identification of reference genes for RT-qPCR data normalization in *Cannabis sativa* stem tissues. Int. J. Mol. Sci. 17. http://dx.doi.org/10.3390/ijms17091556.

Mikshina, P., Chernova, T., Chemikosova, S., Ibragimova, N., Mokshina, N., Gorshkova, T., 2013. Cellulosic Fibers: Role of Matrix Polysaccharides in Structure and Function. http://dx.doi.org/10.5772/51941.

Moreira-Vilar, F.C., Siqueira-Soares, R., de, C., Finger-Teixeira, A., de Oliveira, D.M., Ferro, A.P., da Rocha, G.J., Ferrarese Mde, L., dos Santos, W.D., Ferrarese-Filho, O., 2014. The acetyl bromide method is faster, simpler and presents best recovery of lignin in different herbaceous tissues than klason and thioglycolic acid methods. PLoS One 9, e110000. http://dx.doi.org/10.1371/journal.pone.0110000.

Pinelli, P., Ieri, F., Vignolini, P., Bacci, L., Baronti, S., Romani, A., 2008. Extraction and HPLC analysis of phenolic compounds in leaves, stalks, and textile fibers of *Urtica dioica* L. J. Agric. Food Chem. 56, 9127–9132. http://dx.doi.org/10.1021/jf801552d.

Saldanha, A.J., 2004. Java Treeview—extensible visualization of microarray data. Bioinf. Oxf. Engl. 20, 3246–3248. http://dx.doi.org/10.1093/bioinformatics/bth349.

Tolivia, D., Tolivia, J., 1987. Fasga: a new polychromatic method for simultaneous and differential staining of plant tissues. J. Microsc. 148, 113–117. http://dx.doi.org/10.1111/j.1365-2818.1987.tb02859.x.

Viktorova, J., Jandova, Z., Madlenakova, M., Prouzova, P., Bartunek, V., Vrchotova, B., Lovecka, P., Musilova, L., Macek, T., 2016. Native phytoremediation potential of *Urtica dioica* for removal of PCBs and heavy metals can be improved by genetic manipulations using constitutive CaMV 35S promoter. PLoS One 11, e0167927. http://dx.doi.org/10.1371/journal.pone.0167927.

Zhang, J., Arro, J., Chen, Y., Ming, R., 2013. Haplotype analysis of sucrose synthase gene family in three *Saccharum* species. BMC Genomics 14, 314. http://dx.doi.org/10.1186/1471-2164-14-314.

Zhu, X., Wang, M., Li, X., Jiu, S., Wang, C., Fang, J., 2017. Genome-Wide analysis of the sucrose synthase gene family in grape (*Vitis vinifera*): structure, evolution, and expression profiles. Genes 8. http://dx.doi.org/10.3390/genes8040111.

Zou, C., Lu, C., Shang, H., Jing, X., Cheng, H., Zhang, Y., Song, G., 2013. Genome-wide analysis of the *Sus* gene family in cotton. J. Integr. Plant Biol. 55, 643–653. http://dx.doi.org/10.1111/jipb.12068.